Chapter 1
A Different Catch for Poisson

A. Derya Bakiler, Ali Javili

Abstract Poisson's ratio, similar to other material parameters of isotropic elasticity, is determined via experiments corresponding to small strains. Yet at small-strain linear elasticity, Poisson's ratio has a dual nature; although commonly understood as a *geometrical parameter*, Poisson's ratio is also a *material parameter*. From a geometrical perspective only, the concept of Poisson's ratio has been extended to large deformations by Beatty and Stalnaker. Here, through a variational analysis, we firstly propose an alternative relationship between the Poisson ratio and stretches at finite deformations such that the nature of Poisson's ratio as a material parameter is retained. In doing so, we introduce relationships between the Poisson ratio and stretches at large deformations different than those established by Beatty and Stalnaker. We show that all the nonlinear definitions of Poisson's ratio coincide at the reference configuration and thus, material and geometrical descriptions too coincide, at small-strains linear elasticity. Secondly, we employ this variational approach to bring in the notion of nonlinear Poisson's ratio in peridynamics, for the first time. In particular, we focus on bond-based peridynamics. The nonlinear Poisson's ratio of bond-based peridynamics coincides with 1/3 for two-dimensional and 1/4 for three-dimensional problems, at the reference configuration.

Keywords: Non-linear Poisson's ratio · Variational elasticity · Peridynamics

1.1 Introduction

In its classical definition, that being a kinematic definition in a small deformations context, Poisson's ratio is a constant obtained from the deformation of a domain under uni-axial tension or compression in the axial and lateral directions, illustrated

A. D. Bakiler, A. Javili
Department of Mechanical Engineering, Bilkent University, 06800 Ankara, Turkey
e-mail: derya.bakiler@bilkent.edu.tr, ajavili@bilkent.edu.tr

I. Giorgio et al. (eds.), *Theoretical Analyses, Computations, and Experiments of Multiscale Materials*, Advanced Structured Materials 175,
https://doi.org/10.1007/978-3-031-04548-6_1

in Fig. 1.1. More precisely, it relates to the case where an isotropic domain is subject to an axial strain ε_{ext} in a uni-axial tension test, resulting in the lateral strain ε_{lat}. For the small-strain case the Poisson's ratio definition reads

$$\nu = -\frac{\varepsilon_{\text{lat}}}{\varepsilon_{\text{ext}}}\,, \tag{1.1}$$

which is obviously a *purely geometrical description* in that only geometrical, and not material parameters, are present. The definition of the Poisson ratio (1.1) is the most elementary one. It stems from a purely kinematic stand point, relating the two different resultant strain values of a body, rendering a constant that essentially describes the compressibility of the material. Note that, on the one hand, Poisson's

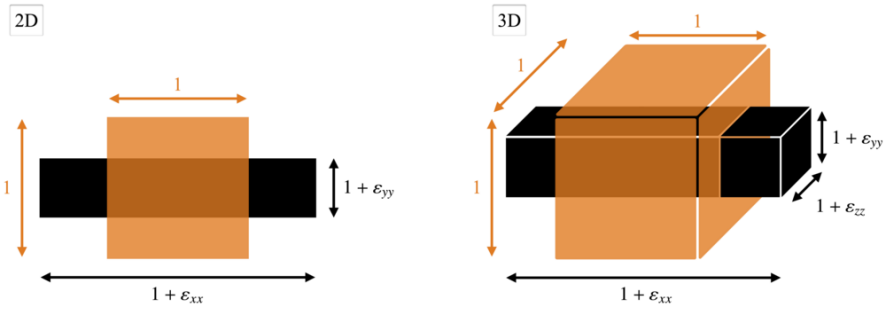

Fig. 1.1 Affine deformation of a unit domain under uni-axial tension test. Lateral deformations occur naturally to minimize the energy, while extension ε_{xx} is a prescribed value.

ratio definition is geometrical in nature and is constant for a material at small strains. On the other hand, from the linear elasticity analysis of isotropic Neo-Hookean materials, one can immediately establish a one-to-one relationship between the geometrical description of Poisson's ratio (1.1) and Lamé parameters as

$$\text{2D} \quad : \quad \nu = \frac{\Lambda}{\Lambda + 2\mu} \qquad , \qquad \text{3D} \quad : \quad \nu = \frac{\Lambda}{2\left[\Lambda + \mu\right]}\,, \tag{1.2}$$

where Λ and μ are the first and second Lamé parameters, respectively. Table 1.1 elucidates the dual nature of Poisson's ratio associated with small-strain linear elasticity. For common (non-auxetic) materials, the Poisson ratio ranges from zero associated with a *fully compressible* material, to $\nu = 0.5$ corresponding to *incompressibility limit* in three-dimensional elasticity. The incompressibility limit for two-dimensional or plane-strain elasticity corresponds to $\nu = 1$, as it can be immediately realized from the geometrical constraints that correspond to a constant area of the domain. Henceforth, for the sake of brevity, we use the term "2D" to represent plane-strain conditions or purely two-dimensional elasticity similar to the interface elasticity theory, see (dell'Isola and Romano, 1987). Poisson's ratio can also take values less than zero, attributed to auxetic materials.

Table 1.1 Poisson's ratio in small-strain linear elasticity and its dual nature as a material parameter (left) or a geometrical definition (right).

	material description		geometrical description				
2D	$\dfrac{\Lambda}{\Lambda+2\mu}$	$=$	ν	$=$	$-\dfrac{\varepsilon_{yy}}{\varepsilon_{xx}}$		
3D	$\dfrac{\Lambda}{2\,[\Lambda+\mu]}$	$=$	ν	$=$	$-\dfrac{\varepsilon_{yy}}{\varepsilon_{xx}}$	$=$	$-\dfrac{\varepsilon_{zz}}{\varepsilon_{xx}}$

Table 1.2 Poisson's ratio at large deformations nonlinear elasticity. The geometrical description of Poisson's ratio has been extended to large deformations (top). We propose an extension of the material description of Poisson's ratio (bottom), via a variational approach. At the reference configuration, both nonlinear variants coincide with their linear counterparts in Table 1.1.

	Beatty & Stalnaker (extension of geometrical description)	
2D	$\nu = -\dfrac{E_{yy}}{E_{xx}}$	$\begin{cases} \boldsymbol{E} = \ln \boldsymbol{U} & m = 0 \\ \boldsymbol{E} = \dfrac{1}{m}[\boldsymbol{U}^m - \boldsymbol{I}] & m \neq 0 \end{cases}$
3D	$\nu = -\dfrac{E_{yy}}{E_{xx}} = -\dfrac{E_{zz}}{E_{xx}}$	

	current approach (extension of material description)				
2D	$\boldsymbol{F} = \mathrm{Diag}(\lambda, \eta)$	&	$\delta\psi = 0$	$\Rightarrow$	$\nu = \nu(\lambda, \eta)$
3D	$\boldsymbol{F} = \mathrm{Diag}(\lambda, \eta, \eta)$	&	$\delta\psi = 0$	$\Rightarrow$	$\nu = \nu(\lambda, \eta)$

Remark on the forthcoming approach to explain the dual nature of Poisson's ratio. *Here, we have started from the elementary, geometrical definition of Poisson's ratio since it is the more established one compared to its material description. Nonetheless, we demonstrate that for linear elasticity, the starting point is preferential because both descriptions of Poisson's ratio render identical results. However, for the rest of the derivations we start from the material definition of Poisson's ratio. This particular approach, as we will see shortly, is motivated by the foresight gained from the large-deformation analysis of the problem.*

1.1.1 Key Objectives

This contribution aims to define Poisson's ratio from a variational perspective. The variational approach at small-strain linear elasticity does not result in new findings. At large deformations, however, it leads to an alternative description of the Poisson ratio, different from those that stem from the commonly accepted approach by Beatty and Stalnaker (1986). In summary, the objective of this contribution is two-fold.

Firstly, we show that the two descriptions of Poisson's ratio, namely the geometrical description (1.1) and the material description (1.2), coincide at small-strain elasticity. We argue that both descriptions can be extended to large deformations. The extension of the geometrical description (1.1) of Poisson's ratio to large deformation elasticity was introduced by Beatty and Stalnaker (1986). In contrast, we suggest an extension of the material description (1.2) to large deformations via a variational approach. The analysis here results in a relationship between the Poisson ratio and stretches at large deformations different than those currently established in the literature on the topic. Table 1.2 summarizes the key features of this contribution associated with Classical Continuum Mechanics (CCM).

Having established the variational formulation to capture Poisson's ratio, in the second part of the contribution, we introduce the notion of nonlinear Poisson's ratio to Peridynamics (PD). We demonstrate that the variational approach established for CMM in the first part can also be adopted to define a nonlinear Poisson's ratio in PD at large deformations. In particular, we focus on bond-based PD, for the sake of simplicity. We show that the nonlinear Poisson's ratio of bond-based PD is not constant, but it coincides with 1/3 for two-dimensional and 1/4 for three-dimensional problems, at the reference configuration.

1.1.2 Notation and Definitions

Direct notation is adopted throughout. Occasional use is made of index notation, the summation convention for repeated indices being implied. The scalar product of two vectors $\boldsymbol{a}$ and $\boldsymbol{b}$ is denoted $\boldsymbol{a} \cdot \boldsymbol{b} = a_i\, b_i$. The scalar product of two second-order tensors $\boldsymbol{A}$ and $\boldsymbol{B}$ is denoted $\boldsymbol{A} : \boldsymbol{B} = A_{ij}\, B_{ij}$. The composition of two second-order tensors $\boldsymbol{A}$ and $\boldsymbol{B}$, denoted $\boldsymbol{A} \cdot \boldsymbol{B}$, is a second-order tensor with components $[\boldsymbol{A} \cdot \boldsymbol{B}]_{ij} = A_{is}\, B_{sj}$. The identity tensor $\boldsymbol{i}$ is denoted as $\boldsymbol{I}$ when it is associated with the material configuration. Trace of a second order tensor $\boldsymbol{A}$ is obtained via its double-contraction with identity, i.e. $\mathrm{Tr}\boldsymbol{A} = \boldsymbol{A} : \boldsymbol{I}$. The fourth-order identity tensor is denoted as $\mathbb{I}$. Similarly, other fourth-order constitutive tensors are also written with the same font, such as $\mathbb{C}$ for the fourth-order constitutive tensor. The tensor product of two second-order tensors $\boldsymbol{A}$ and $\boldsymbol{B}$ is a fourth-order tensor $\mathbb{D} = \boldsymbol{A} \otimes \boldsymbol{B}$ with $D_{ijkl} = A_{ij}\, B_{kl}$. The two non-standard tensor products of two second-order tensors $\boldsymbol{A}$ and $\boldsymbol{B}$ are the fourth-order tensors $[\boldsymbol{A} \overline{\otimes} \boldsymbol{B}]_{ijkl} = A_{ik}\, B_{jl}$ and $[\boldsymbol{A} \underline{\otimes} \boldsymbol{B}]_{ijkl} = A_{il}\, B_{jk}$.

1.1.3 Organization of the Manuscript

The remainder of this contribution is organized as follows. Section 1.2 elaborates on Poisson's ratio in the context of classical continuum mechanics (CCM), and the variational approach that underpins the discussion in this contribution is introduced. Afterwards, this variational framework is employed to formulate a uni-axial tension test for small-strain linear elasticity in Section 1.2.1, resulting in the well-known definitions of the Poisson ratio, for both two-dimensional and three-dimensional elasticity. Section 1.2.2 details on how the developed framework can be employed for large deformation elasticity, resulting in novel definitions for the nonlinear Poisson ratio that mimic the material description of the Poisson ratio rather than its geometrical one. Subsequently, Section 1.3 extends the discussion to Peridynamics (PD) and introduces the notion of a nonlinear Poisson ratio in PD, for the first time. It is shown that the variational approach can be immediately applied to bond-based PD, resulting in a varying Poisson ratio dependent on deformation. Section 1.4 concludes the work and provides further outlook.

1.2 Poisson's Ratio in Classical Continuum Mechanics

In this section, we introduce a variational approach to capture Poisson's ratio in classical continuum mechanics (CCM). To set the stage and convey the idea, we begin with the case of small-strain linear elasticity in Section 1.2.1. We then employ the same variational approach at large deformations nonlinear elasticity in Section 1.2.2. For both discussions on small strains as well as finite deformations, the underlying equation is the equilibrium of a domain under uni-axial tension. Hence, next we formulate equilibrium for the problem at hand.

Under prescribed boundary conditions, equilibrium corresponds to a relaxed state where the deformation field results in the minimum total energy functional. The total energy functional Ψ_{tot} consists of the internal and external contributions denoted Ψ_{int} and Ψ_{ext}, respectively. To minimize Ψ_{tot}, its first variation with respect to deformation, or rather motion, is set to zero as

$$\Psi_{\text{tot}} = \Psi_{\text{int}} + \Psi_{\text{ext}} \quad , \quad \delta\Psi_{\text{tot}} \doteq 0 \quad \Rightarrow \quad \delta\Psi_{\text{tot}} = \delta\Psi_{\text{int}} + \delta\Psi_{\text{ext}} \doteq 0 \,. \tag{1.3}$$

The external energy Ψ_{ext}, in first-order classical continuum mechanics, is essentially minus work as

$$\delta\Psi_{\text{ext}} = -\delta\mathcal{W} \qquad \text{with} \qquad \delta\mathcal{W} = \int_{\mathcal{B}_0} \boldsymbol{b}_0 \cdot \delta\boldsymbol{\varphi} \, \mathrm{d}V + \int_{\partial\mathcal{B}_0} \boldsymbol{t}_0 \cdot \delta\boldsymbol{\varphi} \, \mathrm{d}A \,, \tag{1.4}$$

in which $\mathcal{W}$ denotes the "working", and $\boldsymbol{b}_0$ and $\boldsymbol{t}_0$ are the external body force density and surface force density in the material configuration, respectively. For further details and generalized boundary conditions, see (dell'Isola et al, 2012a,b; Javili et al, 2013; Auffray et al, 2015). The arbitrary variation of motion, denoted as $\delta\boldsymbol{\varphi}$,

is a vector-valued test function $\delta\boldsymbol{\varphi} \in \mathcal{H}_0^1(\mathcal{B}_0)$ that is vanishing where Dirichlet-type boundary conditions are imposed. For a uni-axial tension test which is of interest here, the external body forces are zero and therefore the first integral in Eq. (1.4) vanishes identically. The second integral in Eq. (1.4) vanishes too, since (i) $\delta\boldsymbol{\varphi}$ is zero where displacements are prescribed on the two ends of the domain and (ii) $\boldsymbol{t}_0$ is zero everywhere that a homogeneous Neumann-type boundary condition is imposed. That is, *for the particular problem of a uni-axial tension test*, we seek for the solutions of $\delta\Psi_{\text{int}} = 0$. The internal energy Ψ_{int} reads

$$\Psi_{\text{int}} = \int_{\mathcal{B}_0} \psi \, \mathrm{d}V \,, \tag{1.5}$$

and therefore equilibrium for the current problem reduces to

$$\delta\Psi_{\text{int}} = \int_{\mathcal{B}_0} \delta\psi \, \mathrm{d}V \doteq 0 \,. \tag{1.6}$$

For a uniform deformation in the domain, which holds for a uni-axial tension test, the equilibrium (1.6) then corresponds to

$$\delta\psi \doteq 0 \,. \tag{1.7}$$

The variational constraint (1.7) is an underlying relationship that holds throughout this discussion, and also holds for finite deformations as well as small strains.

1.2.1 Poisson's Ratio for Small-Strain Linear Elasticity

Let $\boldsymbol{\varepsilon}$ be the strain tensor associated with small-strain linear elasticity. In order to establish a variational approach, one needs to begin from the scalar free energy density ψ corresponding to small-strain linear elasticity

$$\psi = \frac{1}{2}\boldsymbol{\varepsilon} : \mathbb{C} : \boldsymbol{\varepsilon} \,, \tag{1.8}$$

with $\mathbb{C}$ being the fourth-order constitutive tensor. The fourth-order constitutive tensor in terms of the first and second Lamé parameters Λ and μ, respectively, reads

$$\mathbb{C} = \mu \left[\boldsymbol{I} \overline{\otimes} \boldsymbol{I} + \boldsymbol{I} \underline{\otimes} \boldsymbol{I} \right] + \Lambda \, \boldsymbol{I} \otimes \boldsymbol{I} \,, \tag{1.9}$$

and therefore

$$\psi = \psi(\boldsymbol{\varepsilon}) = \mu \, \boldsymbol{\varepsilon} : \boldsymbol{\varepsilon} + \frac{1}{2}\Lambda \, \mathrm{Tr}^2 \boldsymbol{\varepsilon} \,. \tag{1.10}$$

Using the relationship (1.2), the free energy density (1.10) in terms of μ and Poisson's ratio ν reads

$$\begin{cases} \text{2D} \quad : \quad \psi = \mu\, \boldsymbol{\varepsilon} : \boldsymbol{\varepsilon} + \dfrac{\mu\nu}{1-\nu} \mathrm{Tr}^2 \boldsymbol{\varepsilon}\,, \\ \text{3D} \quad : \quad \psi = \mu\, \boldsymbol{\varepsilon} : \boldsymbol{\varepsilon} + \dfrac{\mu\nu}{1-2\nu} \mathrm{Tr}^2 \boldsymbol{\varepsilon}\,. \end{cases} \tag{1.11}$$

For a uni-axial tension test in Fig. 1.1, the strain tensor simplifies to a diagonal tensor

$$\text{2D} \ : \ \boldsymbol{\varepsilon} = \mathrm{Diag}(\varepsilon_{xx}, \varepsilon_{yy}) \qquad , \qquad \text{3D} \ : \ \boldsymbol{\varepsilon} = \mathrm{Diag}(\varepsilon_{xx}, \varepsilon_{yy}, \varepsilon_{zz})\,, \tag{1.12}$$

wherein $\varepsilon_{yy} = \varepsilon_{zz}$ is the lateral strain in 3D. Inserting strains (1.12) into the internal energy density (1.11) furnishes

$$\begin{cases} \text{2D} \quad : \quad \psi = \mu\, [\varepsilon_{xx}^2 + \varepsilon_{yy}^2] + \dfrac{\mu\nu}{1-\nu} [\varepsilon_{xx} + \varepsilon_{yy}]^2\,, \\ \text{3D} \quad : \quad \psi = \mu\, [\varepsilon_{xx}^2 + 2\,\varepsilon_{yy}^2] + \dfrac{\mu\nu}{1-2\nu} [\varepsilon_{xx} + 2\,\varepsilon_{yy}]^2\,. \end{cases} \tag{1.13}$$

Next, we set $\delta\psi \doteq 0$ in order to impose equilibrium (1.7). In doing so, note that $\psi = \psi(\varepsilon_{xx}, \varepsilon_{yy})$ and therefore

$$\delta\psi = \frac{\partial \psi}{\partial \varepsilon_{xx}}\, \delta\varepsilon_{xx} + \frac{\partial \psi}{\partial \varepsilon_{yy}}\, \delta\varepsilon_{yy} \doteq 0\,. \tag{1.14}$$

However, for the problem at hand, the extension ε_{xx} is a prescribed quantity and therefore ε_{yy} is the only remaining variable. This immediately results in

$$\delta\psi \doteq 0 \qquad \Rightarrow \qquad \frac{\partial \psi}{\partial \varepsilon_{yy}} \doteq 0\,. \tag{1.15}$$

Finally, we insert the energy densities (1.13) into the *reduced equilibrium equation* (1.15). That is

$$\frac{\partial \psi}{\partial \varepsilon_{yy}} \doteq 0 \quad \Rightarrow \quad \begin{cases} \text{2D} \quad : \quad 2\mu\, \varepsilon_{yy} + \dfrac{2\mu\nu}{1-\nu} [\varepsilon_{xx} + \varepsilon_{yy}] \doteq 0\,, \\ \text{3D} \quad : \quad 2\mu\, \varepsilon_{yy} + \dfrac{2\mu\nu}{1-2\nu} [\varepsilon_{xx} + 2\,\varepsilon_{yy}] \doteq 0\,. \end{cases} \tag{1.16}$$

Solving each relation in Eq. (1.16), results in

$$\text{2D} \quad : \quad \nu = -\frac{\varepsilon_{yy}}{\varepsilon_{xx}} \qquad , \qquad \text{3D} \quad : \quad \nu = -\frac{\varepsilon_{yy}}{\varepsilon_{xx}}\,, \tag{1.17}$$

which shall be compared with Eq. (1.2). That is, *starting from energy, via a variational procedure for a uni-axial tension test, one can show that the material description of Poisson's ratio indeed coincides with its geometrical definition*. This finding per se is not surprising. Nonetheless, as we will see shortly, the same procedure at finite deformations results in relationships for Poisson's ratio that are different from those previously reported in literature.

1.2.2 Poisson's Ratio for Large Deformations Nonlinear Elasticity

Consider the deformation of a continuum body, as illustrated in Fig 1.2. The continuum body occupies the material configuration $\mathcal{B}_0 \subset \mathbb{R}^3$ at time $t = 0$ that is mapped to the spatial configuration $\mathcal{B}_t \subset \mathbb{R}^3$ at any time $t > 0$ via the nonlinear deformation map $\boldsymbol{\varphi}$, with $\boldsymbol{X}$ and $\boldsymbol{x}$ identifying points in the material and spatial configurations, respectively. The deformation gradient in the bulk, denoted $\boldsymbol{F}$, is a linear deformation map that relates an infinitesimal line element $d\boldsymbol{X} \in T\mathcal{B}_0$ to its spatial counterpart $d\boldsymbol{x} \in T\mathcal{B}_t$ via the relation $\mathrm{d}\boldsymbol{x} = \boldsymbol{F} \cdot \mathrm{d}\boldsymbol{X}$ where $\boldsymbol{F} := \mathrm{Grad}\boldsymbol{\varphi}$.

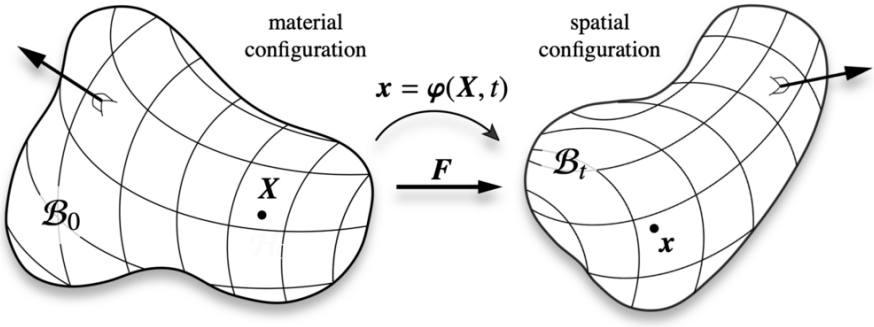

Fig. 1.2 The deformation of a continuum body which occupies the material configuration $\mathcal{B}_0 \subset \mathbb{R}^3$ at time $t = 0$ that is mapped to the spatial configuration $\mathcal{B}_t \subset \mathbb{R}^3$ at any time $t > 0$ via the nonlinear deformation map $\boldsymbol{\varphi}$.

For large deformations, and from a geometrical perspective, the Poisson ratio can still be expressed as minus the ratio of lateral strain to extensional strain, similar to small-strain linear elasticity, if the strain measures themselves correspond to large deformations. That is

$$\nu = -\frac{\text{lateral strain}}{\text{extensional strain}} \qquad \text{with} \qquad \text{strain} \equiv \text{any finite strain measure}\,, \tag{1.18}$$

holds intuitively as an extension of the geometrical description of Poisson's ratio to finite strains. This case has been first explored by Beatty and Stalnaker (1986), who essentially constructed the general definition for nonlinear Poisson's ratio (1.18). In its original definition, extensional and lateral strains were the (Biot) strain measures $E_{xx} = \lambda - 1$ and $E_{yy} = \eta - 1$, respectively, with λ and η being the extensional and lateral stretches, respectively, associated with a uni-axial tension test. Nonetheless, the term "strain" can be extended to a larger Seth-Hill family of strain functions, collectively expressed as

$$\boldsymbol{E}(\boldsymbol{U}) = \begin{cases} \ln \boldsymbol{U} & \text{if} \quad m = 0\,, \\ \dfrac{1}{m}\left[\boldsymbol{U}^m - \boldsymbol{I}\right] & \text{if} \quad m \neq 0\,, \end{cases} \tag{1.19}$$

with $\boldsymbol{U}$ being the (right) stretch tensor. In particular, the most commonly used strain measures are

$$\begin{aligned} m=1 \quad &\Rightarrow \quad \text{Biot} \quad : \quad \boldsymbol{E}_B = \boldsymbol{U} - \boldsymbol{I}\,, \\ m=0 \quad &\Rightarrow \quad \text{Hencky} \quad : \quad \boldsymbol{E}_H = \ln \boldsymbol{U}\,, \\ m=2 \quad &\Rightarrow \quad \text{Green} \quad : \quad \boldsymbol{E}_G = \tfrac{1}{2}\,[\boldsymbol{U}^2 - \boldsymbol{I}]\,, \\ m=-2 \quad &\Rightarrow \quad \text{Almansi} \quad : \quad \boldsymbol{E}_A = -\tfrac{1}{2}\,[\boldsymbol{U}^{-2} - \boldsymbol{I}]\,. \end{aligned} \tag{1.20}$$

Obviously, the definition (1.18) is in essence the same as the previously mentioned Poisson ratio measure for linear, small deformations. What makes this case different is that for finite deformations, there is not a single measure for strain. Hence every strain measure renders a different definition of nonlinear Poisson ratio. This prohibits us from directly equating the two kinematic measures of Poisson's ratio associated with Eq. (1.1) and Eq. (1.18). For instance, for the most commonly used strain measures, the nonlinear Poisson ratio reads

$$\begin{aligned} &\text{Biot} \quad : \quad \nu = \frac{1-\eta}{\lambda - 1} \quad , \quad \text{Hencky} \quad : \quad \nu = -\frac{\ln \eta}{\ln \lambda}\,, \\ &\text{Green} \quad : \quad \nu = \frac{1-\eta^2}{\lambda^2 - 1} \quad , \quad \text{Almansi} \quad : \quad \nu = \frac{1-\eta^{-2}}{\lambda^{-2} - 1}\,. \end{aligned} \tag{1.21}$$

Note that in all the definitions (1.21), but also throughout this contribution, λ and η denote the extensional and lateral stretches, respectively, associated with the deformation gradient

$$\text{2D} \;:\; \boldsymbol{F} = \text{Diag}(\lambda, \eta) \quad , \quad \text{3D} \;:\; \boldsymbol{F} = \text{Diag}(\lambda, \eta, \zeta)\,, \tag{1.22}$$

wherein $\zeta = \eta$ is the lateral stretch in 3D. Notice that we now have a definition for a nonlinear Poisson's ratio where the Poisson's ratio is not simply a constant for a given material, but changes according to the stretch applied to the material.

Now moving onto the material description in a nonlinear setting, we employ the variational approach established previously. To do so, we begin from a (polyconvex) hyperelastic free energy density $\psi = \psi(\boldsymbol{F})$. For instance, for a compressible Neo-Hookean model ψ reads

$$\psi = \psi(\boldsymbol{F}) = \frac{1}{2}\,\mu\,[\boldsymbol{F} : \boldsymbol{F} - 3 - 2\ln J] + \Lambda\,[\,\frac{1}{4}\,[J^2 - 1] - \frac{1}{2}\,\ln J\,]\,, \tag{1.23}$$

where $\boldsymbol{F}$ is the deformation gradient defined previously, and $J := \text{Det}\boldsymbol{F}$. The free energy density (1.23) shall be compared with its counterpart (1.10) for small-strain linear elasticity. Analogous to what was established in Section 1.2.1, using the relationship (1.2), the free energy density in terms of μ and Poisson's ratio ν reads

$$\begin{cases} \text{2D} \;:\; \psi = \dfrac{1}{2}\,\mu\,[\boldsymbol{F}:\boldsymbol{F} - 2 - 2\ln J] + \dfrac{2\mu\nu}{1-\nu}\,[\,\dfrac{1}{4}\,[J^2-1] - \dfrac{1}{2}\,\ln J\,]\,, \\ \text{3D} \;:\; \psi = \dfrac{1}{2}\,\mu\,[\boldsymbol{F}:\boldsymbol{F} - 3 - 2\ln J] + \dfrac{2\mu\nu}{1-2\nu}\,[\,\dfrac{1}{4}\,[J^2-1] - \dfrac{1}{2}\,\ln J\,]\,. \end{cases} \tag{1.24}$$

For a uni-axial tension test, the deformation gradient $\boldsymbol{F}$ simplifies to a diagonal tensor expressed in Eq. (1.22). Inserting the corresponding deformation gradient (1.22) into the internal energy density (1.24) furnishes

$$\begin{cases} \text{2D} \;: & \psi = \dfrac{1}{2}\,\mu\,\left[\lambda^2+\eta^2-2-2\ln(\lambda\eta)\right] \\ & \qquad + \dfrac{2\mu\nu}{1-\nu}\,[\,\dfrac{1}{4}\,[(\lambda\eta)^2-1] - \dfrac{1}{2}\,\ln(\lambda\eta)\,]\,, \\ \text{3D} \;: & \psi = \dfrac{1}{2}\,\mu\,\left[\lambda^2+2\eta^2-3-2\ln(\lambda\eta^2)\right] \\ & \qquad + \dfrac{2\mu\nu}{1-2\nu}\,[\,\dfrac{1}{4}\,[(\lambda\eta^2)^2-1] - \dfrac{1}{2}\,\ln(\lambda\eta^2)\,]\,. \end{cases} \tag{1.25}$$

Next, we set $\delta\psi \doteq 0$ in order to impose equilibrium (1.7). In doing so, note that $\psi = \psi(\lambda,\eta)$ and therefore

$$\delta\psi = \frac{\partial\psi}{\partial\lambda}\,\delta\lambda + \frac{\partial\psi}{\partial\eta}\,\delta\eta \doteq 0\,. \tag{1.26}$$

However, for the problem at hand, the extension λ is a prescribed quantity and therefore η is the only remaining variable. This immediately results in

$$\delta\psi \doteq 0 \qquad \Rightarrow \qquad \frac{\partial\psi}{\partial\eta} \doteq 0\,. \tag{1.27}$$

Finally, we use the energy densities (1.25) in the *reduced equilibrium equation* (1.27). That is

$$\frac{\partial\psi}{\partial\eta} \doteq 0 \quad \Rightarrow \quad \begin{cases} \text{2D} \;:\; \dfrac{1}{2}\,\mu\left[2\eta - \dfrac{2}{\eta}\right] + \dfrac{2\mu\nu}{1-\nu}\left[\dfrac{1}{2}\lambda^2\eta - \dfrac{1}{2\eta}\right] \doteq 0\,, \\ \text{3D} \;:\; \dfrac{1}{2}\,\mu\left[4\eta - \dfrac{4}{\eta}\right] + \dfrac{2\mu\nu}{1-2\nu}\left[\lambda^2\eta^3 - \dfrac{1}{\eta}\right] \doteq 0\,. \end{cases} \tag{1.28}$$

Solving each relation in Eq. (1.28), results in

$$\text{2D} \quad : \quad \nu = \frac{1-\eta^{-2}}{1-\lambda^2} \qquad , \qquad \text{3D} \quad : \quad \nu = \frac{1-\eta^{-2}}{2-\eta^{-2}-\lambda^2\eta^2}\,, \tag{1.29}$$

which shall be compared with Eq. (1.21). That is, *for large deformations too, starting from energy, via a variational procedure for a uni-axial tension test, one can establish a material description of Poisson's ratio that no longer coincides with its commonly*

accepted geometrical definitions. Table 1.3 extends Table 1.2 and summarizes the aspects of Poisson's ratio at large deformations.

Table 1.3 Poisson's ratio at large deformations nonlinear elasticity. The geometrical description of Poisson's ratio has been extended to large deformations (top). Via a variational approach, we propose an extension of the material description of Poisson's ratio (bottom).

	Beatty & Stalnaker	
2D	$\nu = -\dfrac{E_{yy}}{E_{xx}}$	$\begin{cases} \boldsymbol{E} = \ln \boldsymbol{U} & m = 0 \\ \boldsymbol{E} = \dfrac{1}{m}[\boldsymbol{U}^m - \boldsymbol{I}] & m \neq 0 \end{cases}$
3D	$\nu = -\dfrac{E_{yy}}{E_{xx}} = -\dfrac{E_{zz}}{E_{xx}}$	

2D	Biot : $\nu_B = \dfrac{1-\eta}{\lambda - 1}$	Hencky : $\nu_H = -\dfrac{\ln \eta}{\ln \lambda}$
3D	Green : $\nu_G = \dfrac{1-\eta^2}{\lambda^2 - 1}$	Almansi : $\nu_A = \dfrac{1-\eta^{-2}}{\lambda^{-2} - 1}$

	current approach
2D	$\boldsymbol{F} = \mathrm{Diag}(\lambda, \eta) \quad \& \quad \delta\psi = 0 \quad \Rightarrow \quad \nu = \nu(\lambda, \eta)$
3D	$\boldsymbol{F} = \mathrm{Diag}(\lambda, \eta, \eta) \quad \& \quad \delta\psi = 0 \quad \Rightarrow \quad \nu = \nu(\lambda, \eta)$

2D	$\nu = \dfrac{1-\eta^{-2}}{1-\lambda^2}$
3D	$\nu = \dfrac{1-\eta^{-2}}{2-\eta^{-2}-\lambda^2\eta^2}$

Fig. 1.3 illustrates the different kinematic measures of Poisson's ratio, namely that of Biot, Hencky, Green and Almansi, as gathered in Eq. (1.21), at the incompressibility limit, against the current kinetic definition (1.29). The nonlinear Poisson ratio ν, obtained for the various definitions, is plotted versus the axial stretch λ, which ranges from 0.5 to 1.5, thus covering both contraction and extension. Clearly, all of the definitions coincide at $\lambda = 1$, to the expected, incompressible value of $\nu = 1$ for 2D and $\nu = \frac{1}{2}$ for 3D. The significance of this point lies in the fact that deformations close to $\lambda = 1$ correspond to small stains. Hence as we move away from this small-strain

limit, the geometrical and material descriptions of Poisson's ratio move away from each other, since the nonlinearity of the Poisson ratio becomes more pronounced and consequently, the different functions begin to portray different behaviors. Only the current definition and the Hencky definition at the incompressibility limit remain constant regardless of the stretch λ.

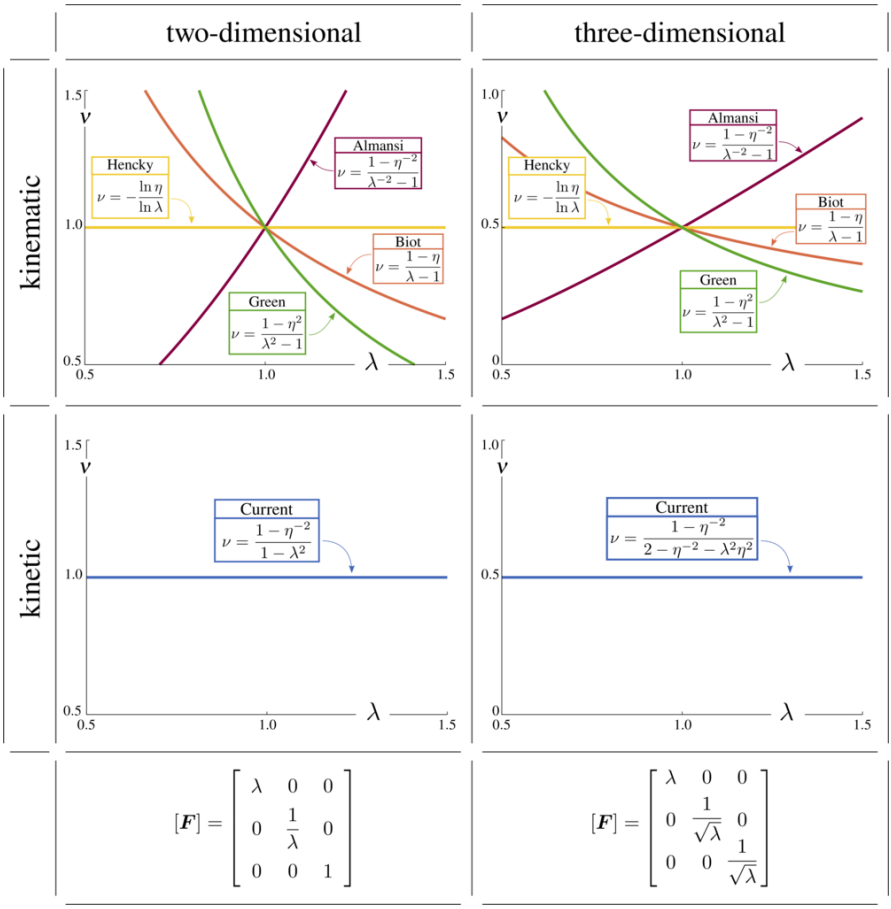

Fig. 1.3 Comparison of the current kinetic nonlinear Poisson's ratio definition with previously established, kinematic definitions.

Equipped with the nonlinear Poisson's ratio (1.29), another interesting aspect to investigate is the relationship between the lateral stretch η and the Jacobian J. This combination is particularly intriguing since $J = \mathrm{Det}\boldsymbol{F}$ is the ratio of the current over reference volume of the domain for 3D and the ratio of the current over reference area of the domain for 2D. Therefore J serves as an indication of compressibility of a material too. That is, for nearly incompressible materials we expect $J \to 1$.

In doing so, it proves helpful to define a dimensionless "compressibility parameter" $\alpha = \Lambda/2\mu$, with α ranging from 0 at full compressibility, to $\alpha \to \infty$ at the incompressibility limit. Using the relationships established for the nonlinear Poisson ratio (1.29), we can immediately see that α boils down to the same function in terms of η and J, for both 2D and 3D. That is

$$\alpha = \frac{\Lambda}{2\,\mu} \quad \Rightarrow \quad \left\{ \begin{array}{l} \text{2D} \;:\; \alpha = \dfrac{\nu}{1-\nu} \\ \\ \text{3D} \;:\; \alpha = \dfrac{\nu}{1-2\nu} \end{array} \right\} \quad \Rightarrow \quad \alpha = \frac{1-\eta^2}{J^2-1}\,. \tag{1.30}$$

Therefore, it is possible to express the lateral stretch η as a function of the compressibility parameter α and the Jacobian J, where for a uni-axial tension test, $J = \lambda\eta$ in 2D and $J = \lambda\eta^2$ in 3D. That is

$$\eta = \sqrt{1 - \alpha\,[J^2 - 1]}\,. \tag{1.31}$$

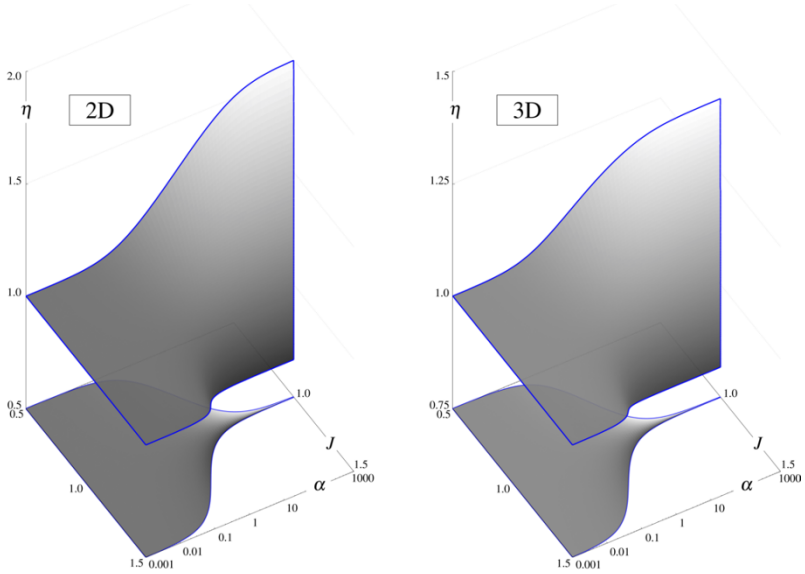

Fig. 1.4 Illustration of the lateral stretch η versus Jacobian J and compressibility parameter α for 2D (left) and 3D (right). As we move towards full incompressibility, J converges to 1, as expected.

Even though the definition (1.31) is obtained through a variational approach associated with the material description of the Poisson ratio, the geometrical interpretation of it is still visible. As the domain becomes increasingly compressible, this suggests geometrically that no matter what the axial stretch, λ is, there would be close to no contraction in the lateral direction, corresponding to $\eta \to 1$. This is clearly seen in Fig. 1.4, for both 2D (left) and 3D (right), with the curve flattening and

converging to a single value of $\eta = 1$, regardless of J hence of λ, as $\alpha \to 0$. On the other hand, as the material gets more and more incompressible with increasing α, the range of admissible values for η increases. Additionally, as we move towards full incompressibility, since at full incompressibility the volume is preserved, J converges to 1. We also see that the whole range of η becomes viable at the incompressible limit. This stems from the fact that incompressibility dictates that $J = 1$ and therefore $\eta = 1/\lambda$ in 2D, or $\eta = 1/\sqrt{\lambda}$ in 3D, which shows that for any value of axial stretch λ there exists a solution for the lateral stretch η to ensure incompressibility.

Remark on generalizing the methodology. *The variational framework here to extend the material description of Poisson's ratio to large deformations was carried out so far for the hyperelastic free energy density (1.23). This particular choice of (Ogden) free energy density was only made to simplify the derivations and highlights the key features of the procedure while avoiding technical complexities. Nonetheless, the developed framework itself is generic and can be applied to any other free energy density of an elastic material. That is, while the nonlinear Poisson ratio (1.29) is exclusively derived for the free energy density (1.23), it can be shown that any $\psi = \psi(\boldsymbol{F} : \boldsymbol{F}, J)$ furnishes a relationship between λ, η and ν akin to the nonlinear Poisson ratio (1.29). Generalizing even further, the framework can also be applied to any isotropic free energy density $\psi = \psi(I_1, I_2, I_3)$ with $I_1 := \mathrm{Tr}\,\boldsymbol{C}$, $I_2 := \mathrm{Tr}\,\mathrm{Cof}\,\boldsymbol{C}$ and $I_3 := \mathrm{Det}\,\boldsymbol{C}$ being the three principal invariants of the right Cauchy–Green tensor $\boldsymbol{C}$.*

Remark on the utility of the nonlinear Poisson's ratio. *One application of the nonlinear Poisson definition developed herein lies in understanding the instability behavior of soft, compressible materials under plane deformations. Instabilities that occur when a domain under compression buckles at a certain point to release energy have found several applications and are ubiquitous in nature. However, until recently, the large deformation instability analysis of a compressible domain under compression had not been thoroughly carried out. For instance, it is well-established that an incompressible half-space reaches instability at the critical stretch of $\lambda = 0.544$, referred to as Biot instability. However, with the use of a compressible material model, such as (1.23), imposing the uniform deformation related to uni-axial compression yields the nonlinear Poisson ratio (1.29). The nonlinear Poisson ratio can then be employed to solve for the critical stretch at which bifurcation occurs, showing that the critical stretch ranges from $\lambda = 0.486$ at full compressibility to $\lambda = 0.544$ at the incompressible limit. This utility is valid since, unlike the commonly accepted definitions of nonlinear Poisson's ratio, in our approach at large deformations too the Poisson's ratio is retained as a material parameter .*

1.3 Poisson's Ratio in Peridynamics

Peridynamics (PD) established by Silling (2000), following the pioneering works of Piola (dell'Isola et al, 2015, 2017), is a non-local continuum mechanics theory. In PD, the behavior of each material point is dictated by its interactions with other material points in its vicinity. Various applications and extensions of PD have been investigated in the past two decades. For a brief description of PD together with a review of its applications and related studies in different fields to date, see (Javili et al, 2019) and the references therein. Similar to the variational approach developed in Section 1.2, via minimizing the internal energy density, the Poisson ratio of bond-based peridynamics is investigated next.

Again, consider the deformation of a continuum body that is mapped from the material configuration $\mathcal{B}_0$ to the spatial configuration $\mathcal{B}_t$ via the nonlinear deformation map $\boldsymbol{\varphi}$, as illustrated in Fig. 1.5. Here also, $\boldsymbol{X}$ and $\boldsymbol{x}$ identify points in the material

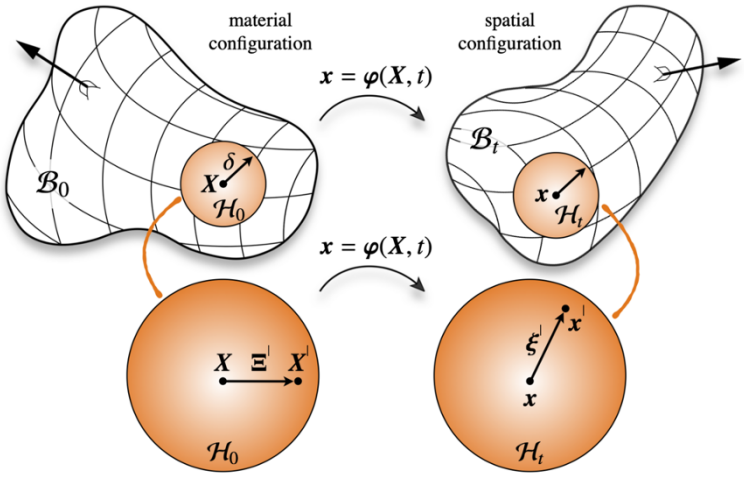

Fig. 1.5 Motion of a continuum body within the PD formulation. The neighborhood of $\boldsymbol{X}$ is mapped to the neighborhood of $\boldsymbol{x}$.

and spatial configurations, respectively. The non-locality assumption of PD dictates that any point $\boldsymbol{X}$ in the material configuration can interact with other points $\boldsymbol{X}'$ within its horizon $\mathcal{H}_0(\boldsymbol{X})$. The *measure* of the horizon in the material configuration, denoted as δ, is generally the radius of a spherical neighborhood at $\boldsymbol{X}$. The relative positions between a point and its neighbors are denoted by $\boldsymbol{\Xi}'$ and $\boldsymbol{\xi}'$ in the material and spatial configurations, respectively. That is

$$\boldsymbol{\Xi}' := \boldsymbol{X}' - \boldsymbol{X} \quad , \qquad \boldsymbol{\xi}' := \boldsymbol{x}' - \boldsymbol{x} \, .$$

The bond stretch $S^{\shortmid}$ is defined by $S^{\shortmid} = l^{\shortmid}/L^{\shortmid}$ with $L^{\shortmid} := |\boldsymbol{\Xi}^{\shortmid}|$ and $l^{\shortmid} := |\boldsymbol{\xi}^{\shortmid}|$ where $L^{\shortmid}$ and $l^{\shortmid}$ are the bond lengths in the material and spatial configurations respectively.

For an affine deformation, with a linear deformation map $\boldsymbol{F}$ between the line elements $\mathrm{d}\boldsymbol{\Xi}^{\shortmid} \in T\mathcal{B}_0$ and $\mathrm{d}\boldsymbol{\xi}^{\shortmid} \in T\mathcal{B}_t$, the mapping reads

$$\mathrm{d}\boldsymbol{\xi}^{\shortmid} = \boldsymbol{F} \cdot \mathrm{d}\boldsymbol{\Xi}^{\shortmid} \quad , \qquad \Rightarrow \qquad \boldsymbol{\xi}^{\shortmid} = \boldsymbol{F} \cdot \boldsymbol{\Xi}^{\shortmid} \, . \tag{1.32}$$

Of particular interest for this contribution is the deformation map $\boldsymbol{F}$ associated with a uni-axial tension test, illustrated in Fig. 1.6. In order to compute the Poisson ratio

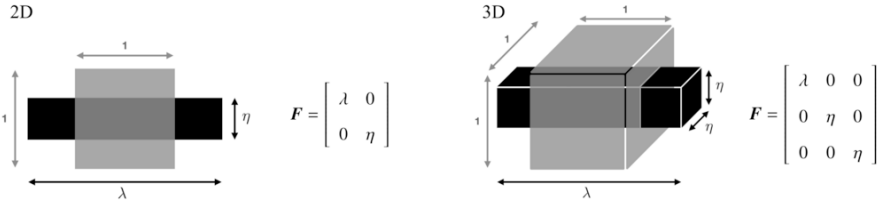

Fig. 1.6 Affine deformation of a unit domain via the linear deformation map $\boldsymbol{F}$, for 2D (left) and 3D (right). The prescribed deformation represents a uni-axial tension test. Extensional and lateral stretches are denoted as λ and η, respectively.

associated with the bond-based PD, we follow the same variational argument in Section 1.2. That is, we minimize the internal energy density via imposing $\delta\psi = 0$. In contrast to CCM, however, the free energy density ψ itself is an integral over the horizon.

For a two-dimensional domain, the internal energy density of PD per unit *area* in the material configuration is the integral of its density $\psi^{\shortmid}$ over the horizon $\mathcal{H}_0$. Similarly, for a three-dimensional domain, the internal energy density of PD per unit *volume* in the material configuration is the integral of its density $\psi^{\shortmid}$ over the horizon $\mathcal{H}_0$. Accordingly, $\psi^{\shortmid}$ is the internal energy density per *area* squared for 2D and per *volume* squared for 3D in the material configuration. That is

$$\text{2D} \quad : \quad \psi = \frac{1}{2}\int_{\mathcal{H}_0} \psi^{\shortmid} \, \mathrm{d}A^{\shortmid} \qquad , \qquad \text{3D} \quad : \quad \psi = \frac{1}{2}\int_{\mathcal{H}_0} \psi^{\shortmid} \, \mathrm{d}V^{\shortmid} \, . \tag{1.33}$$

wherein the factor one-half before the integral is introduced to prevent double-counting since the combination of each pair of points within the horizon occurs twice when going over the global integral. This means that for each pair of points A and B, the pair-wise energy density gets counted twice, one from the sum over point A, and once from the sum over point B. The density of the internal energy density $\psi^{\shortmid}$ is commonly expressed via a harmonic potential with a bond constant C. Therefore

$$\psi^{\mid} = \frac{1}{2}\, C\, L^{\mid}\, [\, S^{\mid} - 1\,]^2 \;\Rightarrow\; \begin{cases} \text{2D} \;:\; \psi = \dfrac{1}{2}\displaystyle\int_{\mathcal{H}_0} \frac{1}{2}\, C\, L^{\mid}\, [\, S^{\mid} - 1\,]^2 \, \mathrm{d}A^{\mid}\,, \\[2ex] \text{3D} \;:\; \psi = \dfrac{1}{2}\displaystyle\int_{\mathcal{H}_0} \frac{1}{2}\, C\, L^{\mid}\, [\, S^{\mid} - 1\,]^2 \, \mathrm{d}V^{\mid}\,. \end{cases} \tag{1.34}$$

The bond-based interaction energy density (1.34) of PD shall be compared with its counterpart (1.24) in CCM. Therefore, for the uni-axial tension test of interest here, the internal energy density ψ reads

$$\begin{cases} \text{2D} \;:\; \psi = \dfrac{1}{2}\displaystyle\int_{\mathcal{H}_0} \frac{1}{2}\, C\, |\boldsymbol{\Xi}^{\mid}|\, \big[\, \frac{|\boldsymbol{F}\cdot\boldsymbol{\Xi}^{\mid}|}{|\boldsymbol{\Xi}^{\mid}|} - 1\,\big]^2 \, \mathrm{d}A^{\mid}\,, \\[2ex] \text{3D} \;:\; \psi = \dfrac{1}{2}\displaystyle\int_{\mathcal{H}_0} \frac{1}{2}\, C\, |\boldsymbol{\Xi}^{\mid}|\, \big[\, \frac{|\boldsymbol{F}\cdot\boldsymbol{\Xi}^{\mid}|}{|\boldsymbol{\Xi}^{\mid}|} - 1\,\big]^2 \, \mathrm{d}V^{\mid}\,. \end{cases} \tag{1.35}$$

wherein $\boldsymbol{F} = \mathrm{Diag}(\lambda, \eta)$ for 2D and $\boldsymbol{F} = \mathrm{Diag}(\lambda, \eta, \eta)$ for 3D.

Next, we evaluate the internal energy densities (1.35) and identify their minimum to obtain a relationship between the lateral contraction η and the prescribed extensional stretch λ. More specifically, via setting $\delta\psi = 0$, we compute a nonlinear Poisson's ratio associated with bond-based PD. In doing so, similar to the discussion in Section 1.2.2, we recall $\psi = \psi(\lambda, \eta)$ and therefore

$$\delta\psi = \frac{\partial\psi}{\partial\lambda}\,\delta\lambda + \frac{\partial\psi}{\partial\eta}\,\delta\eta \doteq 0 \qquad \Rightarrow \qquad \frac{\partial\psi}{\partial\eta} \doteq 0\,, \tag{1.36}$$

wherein the last step follows from the fact that for the problem at hand the extension is a prescribed quantity and therefore η is the only remaining variable.

Figures 1.7 and 1.8 illustrate the energy densities (1.35) and its derivative with respect to η, for a wide range of values for λ and η.

Furthermore, these two sets of graphs demonstrate how $\partial\psi/\partial\eta$ varies with respect to the ratio $\frac{1-\eta}{\lambda-1}$ that is of particular interest since it is reminiscent of Biot nonlinear Poisson's ratio. We emphasize, the prescribed longitudinal stretch λ is not necessarily close to one and in fact, it ranges from nearly zero to four for both two-dimensional and three-dimensional cases in the numerical studies here. Clearly, large deformations can lead to Poisson's ratio other than $\frac{1}{3}$ for two-dimensional and other than $\frac{1}{4}$ for three-dimensional problems, associated with bond-based PD.

The nonlinear Poisson's ratio in these graphs follow the Biot definition. Nonetheless, a similar study can be carried out for all the other canonical definitions based on a geometrical interpretation of Poisson's ratio, as well as the material description thereof. With a little mathematical effort, and using L'Hospital's rule if necessary, it can be shown that in the vicinity of the reference configuration, the analysis leads to $\nu = \frac{1}{3}$ for all the canonical definitions of the nonlinear Poisson's ratio, as expected. That is

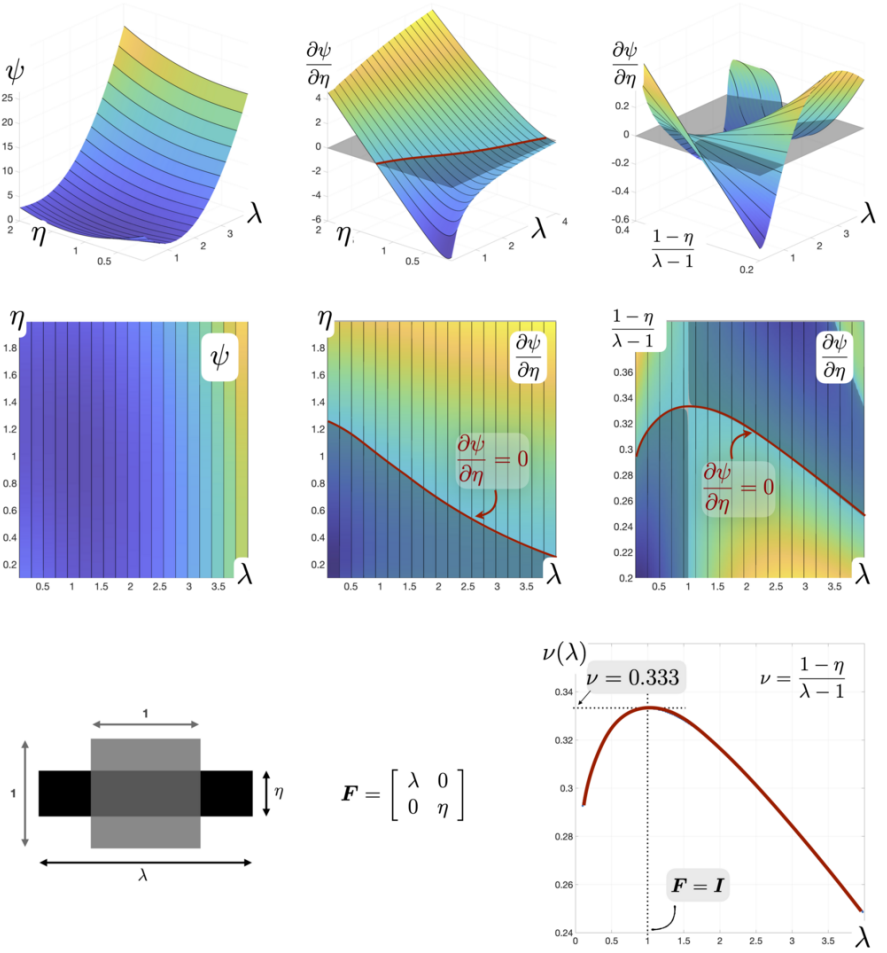

Fig. 1.7 Two-dimensional energy density ψ and its derivative with respect to the lateral stretch η and the ratio $\frac{1-\eta}{\lambda-1}$ for a wide range of values for λ and η. The ratio $\frac{1-\eta}{\lambda-1}$ depends on the stretch λ but approaches $\frac{1}{3}$ as $\lambda \to 1$, as expected. Therefore, one can identify the ratio $\frac{1-\eta}{\lambda-1}$ as a nonlinear Poisson's ratio associated with bond-based peridynamics.

$$\text{if } \frac{1-\eta}{\lambda-1} = \frac{1}{3} \quad \Rightarrow \quad \begin{cases} \text{Biot} & : \quad \nu = \dfrac{1-\eta}{\lambda-1} & \Rightarrow \quad \nu = \dfrac{1}{3}, \\ \text{Hencky} & : \quad \nu = -\dfrac{\ln \eta}{\ln \lambda} & \Rightarrow \quad \nu = \dfrac{1}{3}, \\ \text{Green} & : \quad \nu = \dfrac{1-\eta^2}{\lambda^2-1} & \Rightarrow \quad \nu = \dfrac{1}{3}, \\ \text{Almansi} & : \quad \nu = \dfrac{1-\eta^{-2}}{\lambda^{-2}-1} & \Rightarrow \quad \nu = \dfrac{1}{3}, \\ \text{Current} & : \quad \nu = \dfrac{1-\eta^{-2}}{1-\lambda^2} & \Rightarrow \quad \nu = \dfrac{1}{3}. \end{cases} \tag{1.37}$$

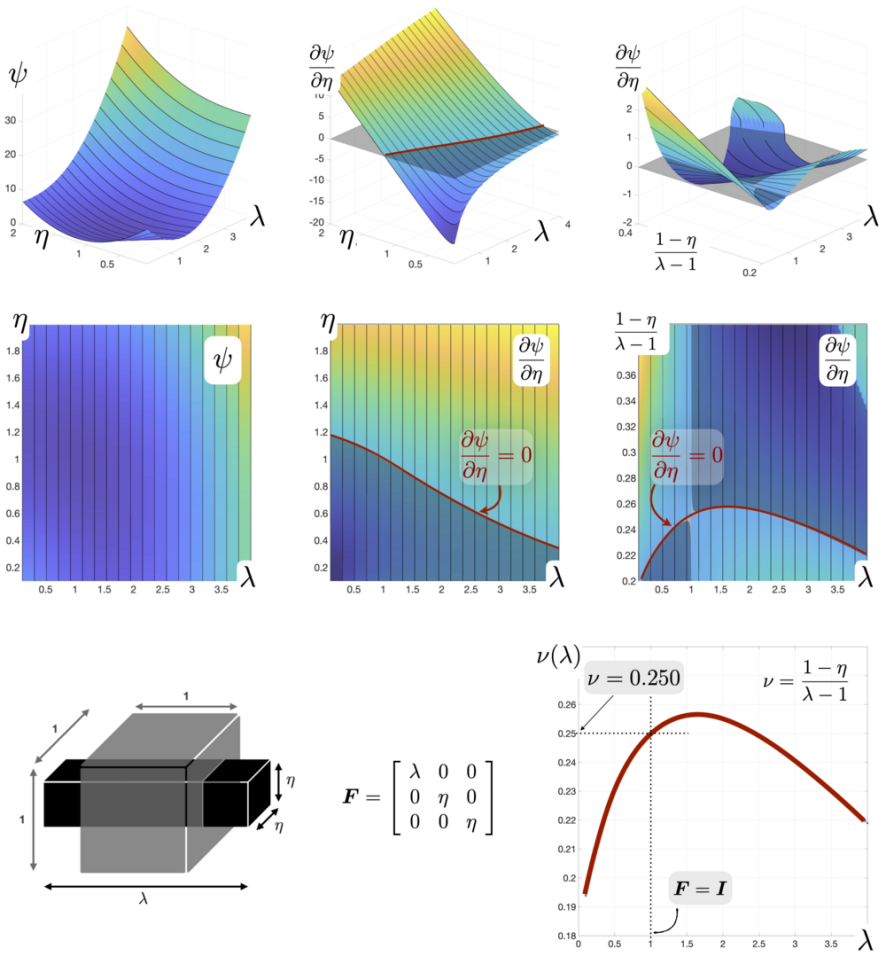

Fig. 1.8 Three-dimensional energy density ψ and its derivative with respect to the lateral stretch η and the ratio $\frac{1-\eta}{\lambda-1}$ for a wide range of values for λ and η. The ratio $\frac{1-\eta}{\lambda-1}$ depends on the stretch λ but approaches $\frac{1}{4}$ as $\lambda \to 1$, as expected. Therefore, one can identify the ratio $\frac{1-\eta}{\lambda-1}$ as a nonlinear Poisson's ratio associated with bond-based peridynamics.

The same conclusion also holds for 3D. More specifically, in the vicinity of the reference configuration, all the canonical definitions of the nonlinear Poisson's ratio coincide at $\nu = \frac{1}{4}$, as expected. That is

$$\text{if } \frac{1-\eta}{\lambda-1}=\frac{1}{4} \;\Rightarrow\; \begin{cases} \text{Biot} & : \quad \nu=\dfrac{1-\eta}{\lambda-1} & \Rightarrow \quad \nu=\dfrac{1}{4}\,, \\ \text{Hencky} & : \quad \nu=-\dfrac{\ln\eta}{\ln\lambda} & \Rightarrow \quad \nu=\dfrac{1}{4}\,, \\ \text{Green} & : \quad \nu=\dfrac{1-\eta^2}{\lambda^2-1} & \Rightarrow \quad \nu=\dfrac{1}{4}\,, \\ \text{Almansi} & : \quad \nu=\dfrac{1-\eta^{-2}}{\lambda^{-2}-1} & \Rightarrow \quad \nu=\dfrac{1}{4}\,, \\ \text{Current} & : \quad \nu=\dfrac{1-\eta^{-2}}{2-\eta^{-2}-\lambda^2\eta^2} & \Rightarrow \quad \nu=\dfrac{1}{4}\,. \end{cases} \tag{1.38}$$

1.4 Conclusion

Among the material parameters of classical first-order linear elasticity, Poisson's ratio stands out in that (i) it is a dimensionless parameter and (ii) it can be interpreted both as a material or a geometrical parameter. Due to its geometrical definition in terms of strains, the Poisson ratio shall be revisited when it comes to large deformations. Beatty and Stalnaker (1986) extended the geometrical interpretation of Poisson's ratio to large deformations. In this contribution, however, we have extended the material description of Poisson's ratio via a variational approach. The variational approach at small strains leads to the trivial outcome that the material and geometrical descriptions of Poisson's ratio coincide. For an example of a hyperelastic material at finite deformations, we have proposed a novel definition for nonlinear Poisson's ratio. Inspired by the findings of the variational approach for classical elasticity, we then employed the same methodology to peridynamics, and in particular, bond-based peridynamics. It is shown that the nonlinear Poisson's ratio of bond-based peridynamics is no longer a constant, but it coincides with 1/3 for two-dimensional and 1/4 for three-dimensional problems, at the reference configuration, as expected. This view can be extended to other formulations of PD and lattice structures. Also, it can be utilized in the up-and-coming field of metamaterial design (Greaves et al, 2011), specifically considering auxetic materials and pantographic structures (Barchiesi et al, 2019; dell'Isola et al, 2019).

References

Auffray N, dell'Isola F, Eremeyev V, Madeo A, Rosi G (2015) Analytical continuum mechanics à la Hamilton-Piola least action principle for second gradient continua and capillary fluids. Mathematics and Mechanics of Solids 20(4):375–417

Barchiesi E, Spagnuolo M, Placidi L (2019) Bending of an infinite beam on an elastic foundation. Mathematics and Mechanics of Solids 24(1):212–234

Beatty M, Stalnaker D (1986) The Poisson function of finite elasticity. Journal of Applied Mechanics, Transactions ASME 53(4):807–813

dell'Isola F, Romano A (1987) On the derivation of thermomechanical balance equations for continuous systems with a nonmaterial interface. International Journal of Engineering Science 25(11-12):1459–1468

dell'Isola F, Madeo A, Placidi L (2012a) Linear plane wave propagation and normal transmission and reflection at discontinuity surfaces in second gradient 3D continua. ZAMM Zeitschrift fur Angewandte Mathematik und Mechanik 92(1):52–71

dell'Isola F, Seppecher P, Madeo A (2012b) How contact interactions may depend on the shape of Cauchy cuts in Nth gradient continua: Approach "à la D'Alembert". Zeitschrift fur Angewandte Mathematik und Physik 63(6):1119–1141

dell'Isola F, Andreaus U, Placidi L (2015) At the origins and in the vanguard of peridynamics, non-local and higher-gradient continuum mechanics: An underestimated and still topical contribution of Gabrio Piola. Mathematics and Mechanics of Solids 20(8):887–928

dell'Isola F, AD C, I G (2017) Higher-gradient continua: The legacy of Piola, Mindlin, Sedov and Toupin and some future research perspectives. Mathematics and Mechanics of Solids 22(4):852–872

dell'Isola F, Seppecher P, Alibert J, Lekszycki T, Grygoruk R, Pawlikowski M, Steigmann D, Giorgio I, Andreaus U, Turco E, Gołaszewski M, Rizzi N, Boutin C, Eremeyev V, Misra A, Placidi L, Barchiesi E, Greco L, Cuomo M, Cazzani A, Corte A, Battista A, Scerrato D, Eremeeva I, Rahali Y, Ganghoffer J, Müller W, Ganzosch G, Spagnuolo M, Pfaff A, Barcz K, Hoschke K, Neggers J, Hild F (2019) Pantographic metamaterials: an example of mathematically driven design and of its technological challenges. Continuum Mechanics and Thermodynamics 31(4):851–884

Greaves G, Greer A, Lakes R, Rouxel T (2011) Poisson's ratio and modern materials. Nature Materials 10(11):823–837

Javili A, dell'Isola F, Steinmann P (2013) Geometrically nonlinear higher-gradient elasticity with energetic boundaries. Journal of the Mechanics and Physics of Solids 61(12):2381–2401

Javili A, Morasata R, Oterkus E, Oterkus S (2019) Peridynamics review. Mathematics and Mechanics of Solids 24(11):3714–3739

Silling S (2000) Reformulation of elasticity theory for discontinuities and long-range forces. Journal of the Mechanics and Physics of Solids 48(1):175–209